Proceedings of ASME Turbo Expo 2022
Turbomachinery Technical Conference and Exposition
GT2022
June 13-17, 2022, Rotterdam, The Netherlands

GT2022-82102

NUMERICAL MODELING OF LEAN SPRAY LIFTED FLAMES IN INCLINED MULTI-BURNER ARRANGEMENTS

Leonardo Langone*, **Matteo Amerighi, Antonio Andreini**
Heat Transfer and Combustion group
Department of Industrial Engineering
University of Florence
via di S.Marta, 3, Florence, Italy 50139

ABSTRACT

Modern combustors operate with lean mixtures to prevent Nitrogen oxides (NOx) formation by limiting the peaks of the temperature inside the combustion chamber. One of the main drawbacks of these technologies is the higher risk of Lean Blow-Off (LBO) compared to the state-of-art Rich Quench Lean combustors. To limit this possibility, combustor designers introduced pioneering concepts for this component. In this fashion, the CHAiRLIFT (Compact Helical Arranged combustoRs with lean LIFTed flames) concept founds its advantages in the structure of the combustion chamber. It combines two concepts: the tilting of the burner's axis relative to the engine axis with a low-swirl lifted spray flame. Here, the combustion can be stabilized at very low equivalence ratios thanks to the interaction between consecutive burners. A numerical analysis was carried out to support the experimental campaign aiming to investigate the performance of the burner under different tilting angles for the burners. Two-phase simulations of the CHAiRLIFT full rig burner were performed in the commercial CFD suite ANSYS Fluent and the results were compared with the available experimental data. Furthermore, a deeper sensitivity to the tilting angle was conducted through the introduction of specific performance parameters to assess the performance and to seek the best promising setup. The outcomes have shown that tilt angles between 20° and 30° could lead to an improvement of the exhaust recirculation, regarding the considered operating conditions.

NOMENCLATURE

c	Progress variable	[-]
h	Step height	[mm]
q	Spread parameter	[-]
S	Swirl number	[-]
Y	Mass fraction	[-]
z	Mixture fraction	[-]
ϕ	Equivalence ratio	[-]
$\dot{\omega}$	Reaction rate	[kg/(m3 s)]
θ	Tilt angle	[deg]

Subscripts

th	Theoretical

Acronyms

CFD	Computational Fluid Dynamics
DPM	Discrete Phase Method
FGM	Flamelet Generated Manifold
IRZ	Inner Recirculation Zone
LBO	Lean Blow-Off
LDI	Lean Direct Injection
LES	Large Eddy Simulation
LOH	Lift-off height
ORZ	Outer Recirculation Zone
PFR	Product Formation Rate
RANS	Reynolds Averaged Navier-Stokes
SHC	Short Helical Combustor
SMD	Sauter Mean Diameter
TAB	Taylor Breakup Analogy

*Address all correspondence to this author: leonardo.langone@htc.unifi.it

INTRODUCTION

The development of highly efficient aircraft engines with low emissions has been the focus of the researcher in the gas turbine combustors field for years. Although important milestones have been reached, further improvements are still needed to avoid dramatic effects on the environment [1]. The respect for the goals set by Flightpath 2050 [2] to cut down 75% of CO2 levels and 90% of current NOx emissions concerning the current standards could be reached only if new technologies will be developed. While pollutants such as carbon monoxide (CO) and unburnt hydrocarbon (UHC) can be handled through the improvement of the combustion efficiency, carbon dioxide (CO2) could be reduced only by improving the fuel consumption, and ultimately by employing alternative fuels and novel engines architectures [3–6]. Furthermore, the other main concern about aircraft pollution is represented by nitrogen oxides (NOx), which are promoted by high pressure and temperature [7]. A strict control of this latter is the key to a reduction of NOx emission and over the years, many strategies have been carried out to this aim. One of the most diffused nowadays among engine manufacturers is represented by Lean Direct Injection (LDI) [8, 9], where fuel and air are premixed in a lean combustion regime before the flame front, avoiding high-temperature spots due to local stoichiometry. The performances of such systems however strongly rely on the operating conditions and the injection system features. On the other hand, these combustion systems are prone to Lean Blow-Off (LBO) occurrences, which are often avoided by employing a pilot injector. In this fashion the combustion stability is increased at the expense of limiting the benefits in terms of NOx. A possible strategy to overcome this issue is represented by the novel combustor concept proposed in the CHAiRLIFT project [10], under the European research program CleanSky2 Joint Undertaking. Here, lean low-swirl lifted spray flames are employed together with a specific layout of the burners assuming a tilted configuration with respect to the engine main axis. In the present work, the combustor of the CHAiRLIFT project is the object of a numerical investigation, aiming to understand the influence of the tilt angle on the reactive process. Firstly, a description of the main features of this combustor architecture is given. Therefore, the adopted numerical modelling is described in detail, especially considering the reactive simulations settings. The numerical results are validated with experimental measurements in terms of temperature field and OH* chemiluminescence available from the related experimental campaign. Then, further tilt angles with respect to the available experimental data are investigated: some comments concerning the overall hot exhaust recirculation are reported aiming to establish which configuration could be optimal for flame stabilization.

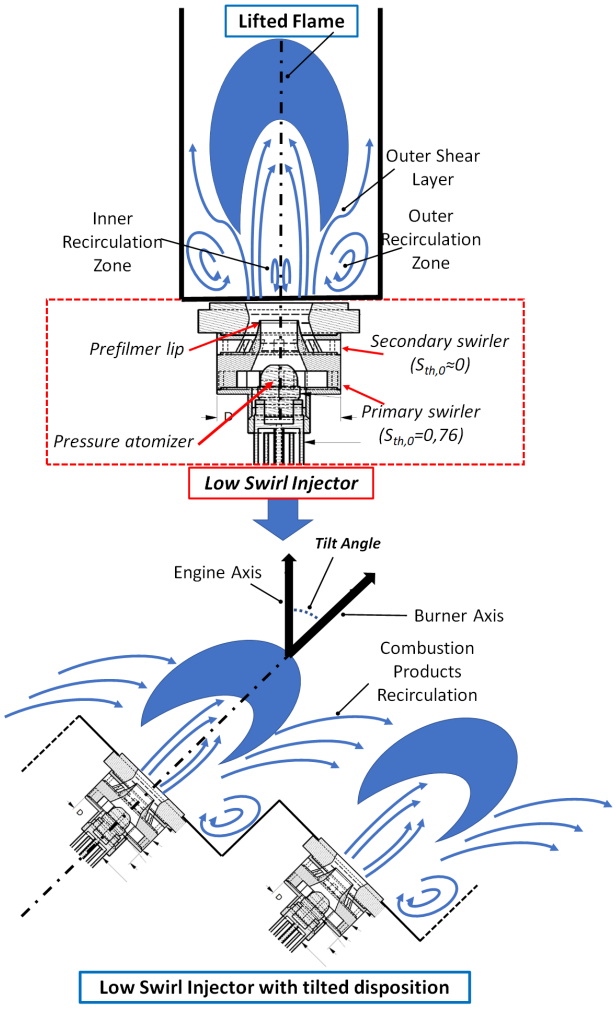

FIGURE 1: CONCEPTUAL SKETCH OF THE CHAiRLIFT ARCHITECTURE.

The CHAiRLIFT project

The CHAiRLIFT acronym stands for *Compact Helical Arranged combustoRs with lean LIFTed Flames*, which resume the main features of such concept: the use of low-swirl flames with an inclined layout of the burners. A conceptual sketch of this architecture can be seen in Fig. 1). Considering the use of low-swirl lifted flames, the major advantage is represented by their potential in NOx emissions reduction and the safety in terms of flashback risk [11, 12]. Their name comes from the reaction zone lifted from the burner exit, allowing a better air-fuel mixing before the flame front, other than limiting the flame-nozzle interactions. Among the possible configurations of low-swirl lifted flames [13, 14], within this project the concept proposed by Zarzalis and investigated at the Engler-Buntler Institut (EBI) of the Karlsruher Institut fur Technologies (KIT) [15, 16] is considered. A double-swirl radial injector derived from an air-blast

atomizer [17] is adopted, where the primary swirler imposes a tangential component to the flow, while the secondary swirl includes only fully radial channels. A relatively weak Inner Recirculation Zone (IRZ) concerning a classic high-swirl injector is therefore established, while high-velocity streams prevent the flame reattachment. The flame stabilization is obtained thanks to the Outer Recirculation Zone (ORZ) derived from the interaction between swirling jet from the nozzle and confinement walls: this is responsible for the upstream transport of hot combustion products from the main reaction zone to the flame base. This phenomenon not only is responsible for the flame stabilization but directly controls the ignition of the incoming fresh mixture. For this reason, the temperature of the recirculating gas is another key parameter for the stabilization of such flames [18] and indeed the flame could not be ignited without confinement walls [19]. Further experimental studies have shown the impact on the operating conditions, which affect the Lift-Off Height (from now on "LOH", meaning the distance between nozzle outlet and flame base) and flame extension [20].

The other key feature of the CHAiRLIFT burner is the inclination of the burners, often referred in the literature as *Short Helical Combustor* (SHC). Burners' axis are tilted by a prescribed angle with respect of the engine axis, so imposing a pre-rotation to the flow and thus the helical flow pattern. The expected advantages regard the possibility to increase the exhaust recirculation among adjacent burners in the annular combustion chamber promoting flame stability. Other important features are the reduction of the combustor length, which help to reduce the overall weight of the engine while improving the structural characteristics. As well, the need for Nozzle Guide Vanes at the turbine inlet is reduced, again contributing to reduce weight and also cooling air requirements. This combustor has been studied widely at the Institut für Thermische Strömungsmaschinen (ITS) of the KIT by Ariabatar [21], with a numerical campaign analysis of the aerothermal characteristics of high-swirl flames. The outcomes point out that a double annular configuration with a tilt angle of 45° leads to the best configuration in terms of gas recirculation and flow pattern at the combustor exit. Also, it has shown that contouring the sidewall could help to reduce the flame deflection. In another study by Hu et al. [22], the effects of the tilt angle for a single annular configuration are investigated. One of the most interesting features is the presence of four different vortex modes depending on the tilt angle. These vortex modes affect the recirculation and the temperature field of the isothermal and the reacting flow. Beyond a specific tilt angle, a further increase is responsible for a reduction of the hot combustion products exchange among the burners. This fact is very important since it highlights the non-linear behavior of the recirculation zones with the tilt angle increase. The CHAiRLIFT concept has been investigated recently by Shamma [23] and Hoffman [24] together with respective coworkers. The numerical study in [24] shown that low-swirl flow strongly interacts with the sidewall of each burner and it experiences a deflection towards this direction due to an asymmetric pressure field. Therefore the angular momentum flux of the helical flow at the combustor outlet is increased compared to the nominal tilt angle of the burners. Other important parameters are the distance of the jet to the sidewall and the position of the inner and outer liners. Hence, the ratio of nozzle diameter to combustor diameter is crucial for the recirculation characteristics. The numerical and experimental study in [23] has confirmed again that unwanted flow deflection of swirled flames with the tilted arrangement is avoided by using low swirl. The most interesting outcome is the remarkable high LBO limits for non-piloted burners, observed for all investigated configurations. The multi-burner configurations were observed to have a superior stability range in contrast to the typical decrease in stability of high swirl multi-burner reported in the literature. Such behaviour could be related to the transfer of hot exhaust gas from the neighboring burner to the flame base of the adjacent burner for the inclined configuration and due to recirculation zones enhancement in in-line configuration, which is essential for the stabilization of the lifted flames.

Operating pressure p_0	101325 Pa
Air inlet temperature T_0	296 K
Nozzle pressure drop $\Delta p_{nozzle}/p_0$	3 %
Equivalence ratio ϕ	0.47

TABLE 1: OPERATING CONDITIONS ADOPTED IN THE NUMERICAL SIMULATIONS.

TEST CASE

The experimental rig here considered is the burner in multi-sector configuration reported in [23]. A linear array consisting of five burners is employed to study the interaction between adjacent flames in terms of flow-field and temperature distribution. To this aim, several configurations are tested in which the burners' axis is inclined of a given tilt angle value θ, to understand how it affects the combustion process when gathered with low-swirl lifted spray flames. For each tilt angle a corresponding axial shift h, which identifies the height of the step, is defined to reproduce the aforementioned effects. Each burner consists of a combustion chamber with a square cross-section of 100x100 mm and an axial extension of 300mm confined by four quartz-glass windows which provide optical access for the measurements in the flame interaction regions. The chamber operates at atmospheric pressure without the presence of any cooling devices, meaning that wall temperature is determined only by the interaction with the hot gas and any possible heat loss occurring through the chamber walls. During the tests, the pressure drop across the

nozzle and the global equivalence ratio could be modified, other than the air preheating at the inlet. The airflow is collected in a plenum before being introduced inside the chamber through nozzles with a nominal effective area of 319 mm^2. This component consists of a primary swirler (8 vanes with 45° inclination) and a secondary swirler (12 vanes with 0° inclination), resulting in a global theoretical swirl number $S_{th,o}$ below 0.4. In the center of the nozzle is placed a pressure atomizer that provides the liquid fuel, JET-A1 in this case, to the prefilmer where the liquid film is formed before being disintegrated. This point marks the beginning of the atomization process, taking place between the two air streams and generating the spray which feeds the main reaction zone. Therefore, fuel and air mix before reaching the flame front, all along with the lift-off distance. Concerning the final section, the test rig is designed to operate with two different configurations of the outlet. In the first one, the flow expands in the ambient without any constraint (refereed as *open case*) while in the second one, an outlet contraction is employed to prevent air ingestion from the surrounding ambient (referred as *contraction case*). Among the available experimental conditions, the specific boundary conditions considered in this numerical work are resumed in Tab. 1. Regarding the experimental measurements, temperature fields maps on the diagonal plane and on the outlet section are available, as well as OH* chemiluminescence maps.

NUMERICAL SETUP

The test rig has been investigated through multiphase reactive simulations of the full-rig for various test rig configurations, summarized in Tab. 2. A set of preliminary simulations on a reduced periodic domain for the Inline configuration has been performed to tune the modelling settings since the effects of the flow deflection are not present. For the sake of brevity, only the final setup adopted on the full rig configuration is here reported. Inline and the 45DEG simulations on the full rig have a twofold target: validate the numerical modelling with the available experimental data and understand the tilt angle effect of the gas recirculation. Then the 20 and 30DEG simulations with the contraction have been performed to investigate and seek the best setup of the burner. The CFD calculations have been conducted with the ANSYS 2019R3 suite: where not specified, the numerical models concerning turbulence, combustion and spray description are reported in [25] together with the related literature references.

Turbulence and Combustion Modelling

Reynolds Average Navier-Stokes (RANS) turbulence context is considered for this numerical work. For all the simulations, the k-ε Realizable model has been used for the turbulence description and its interaction with the chemistry has been modeled with the Flamelet Generated Manifold (FGM). This approach assumes that the combustion takes place in the flamelet regime, therefore the mixing process and the combustion are seen as two separate phenomena, respectively described by two scalars, the mixture fraction z, and the progress variable $c = Y_c/Y_c^{eq}$, where $Y_c = Y_{CO} + Y_{CO_2}$ is the un-normalized progress variable and Y_c^{eq} is its value at equilibrium. A look-up table is obtained by solving a priori number of laminar flames and storing all the possible thermochemical states as a function of the mean values of z and c and their respective variances. Diffusive flamelets have been found to better describe the flames since the low air temperature limits the evaporation in the first part of the combustion chamber, hence the premix of the reactive mixture. The Luche's mechanism [26] consisting of 91 species and 694 reactions has been employed for the chemistry modelling, where the n-decane (NC10H22) is used as a surrogate of the JET-A fuel employed in the experimental tests and Finite Rate closure has been used for the progress variable source term.

Case	θ $[deg]$	h $[mm]$	***Open case***	***Contraction case***
Inline	0	0	•	○
20DEG	20	36.39	○	•
30DEG	30	57.73	○	•
45DEG	45	100	•	•

TABLE 2: TEST RIG CONFIGURATIONS IN THE NUMERICAL INVESTIGATIONS.

Spray Modelling

Injection spray characteristic	
Spray distribution	Rosin-Rammler
SMD	63.5 μm
q	2.23
Cone angle	0 °
Droplet velocity	5 m/s
N° points in radial direction	5
N° points in tangential direction	18

TABLE 3: CHARACTERISTICS OF SPRAY INJECTION.

The Discrete Phase Method (DPM) has been used to track the fuel droplets inside the domain in which the gaseous phase is treated as a continuum whereas the dispersed liquid phase is

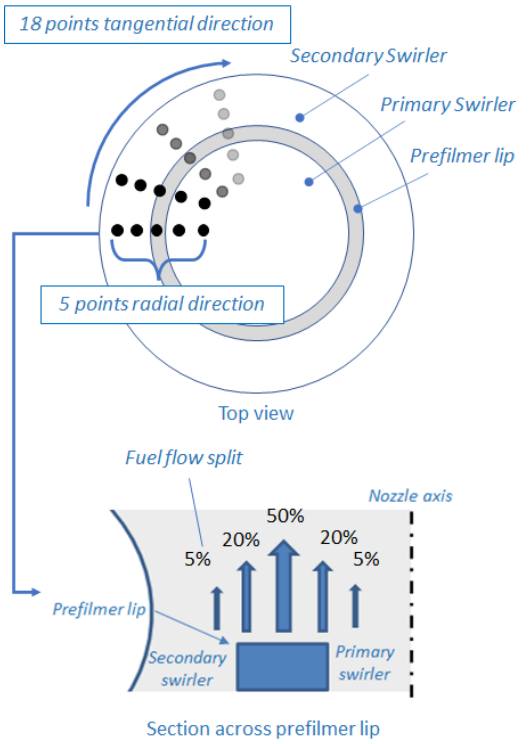

FIGURE 2: CONCEPTUAL SKETCH OF THE INJECTION POINTS POSITION ACROSS THE PREFILMER.

tracked in a Lagrangian framework. The spray boundary conditions have required a large part of this work for their calibration since their impact on the final solution. The liquid fuel injection is considered only from the prefilmer lip, while the whole atomization process along the prefilmer surface has not been included. At this point, it is assumed that the primary breakup of the liquid film is already accomplished. Therefore, the injection has been distributed at several points placed 1.2 mm downstream of the prefilmer lip to reproduce the spray spreading due to the unsteadiness of the flow field. A visualization of the injection points in the proximity of the prefilmer can be seen in Fig.2. The total fuel mass flow rate is derived according to test point equivalence ratio and air mass flow. Additionally, a flow split is applied in the radial direction as 5%-20%-50%-20%-5% of the fuel flow for a given tangential position, from the outermost to innermost point. Each single injection point employs a Rosin-Rammler distribution where the Sauter Mean Diameter SMD and Spread parameter q are derived with a correlation present in literature and suitable for prefilmer atomizer [27]. Droplets are injected with a temperature of 300 K and an initial low velocity, assuming that droplets are rapidly relaxed to the carrier phase velocity. All the mentioned characteristics for the spray injection are resumed in Tab. 3. This procedure has been preliminarily evaluated with the available spray measurements from the previous experimental campaign [15] and it will be further improved once MIE scattering experimental measurements will be available. The discrete and carrier phases are considered with a two-way coupling and secondary breakup has been modeled with the Taylor Breakup Analogy (TAB) model.

Domain and Boundary Conditions

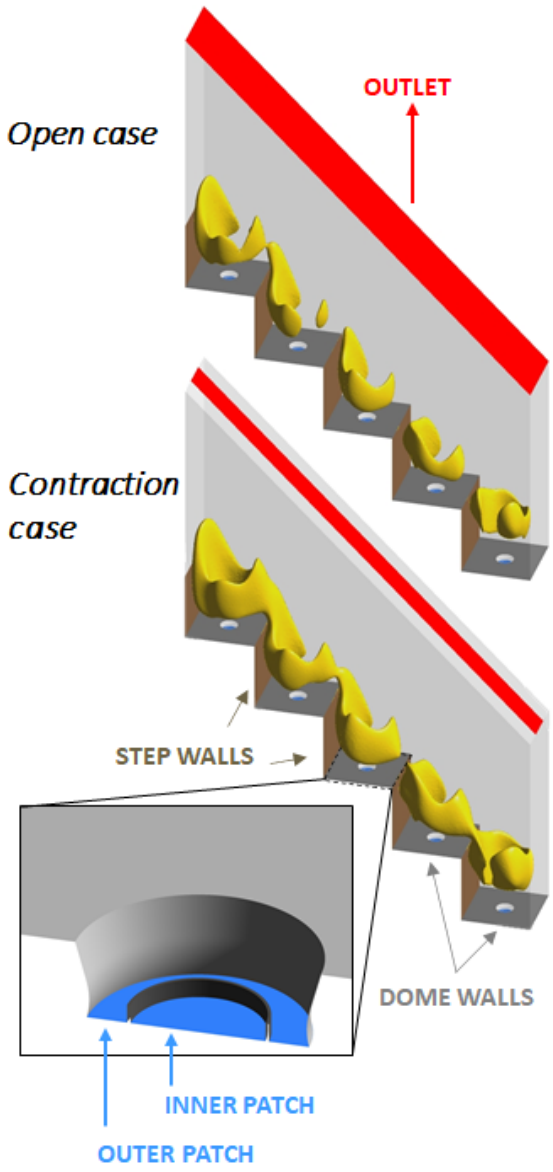

FIGURE 3: COMPUTATIONAL DOMAIN WITH ISO-SURFACE OF PRODUCT FORMATION RATE FOR THE 45DEG CASE WITH AND WITHOUT THE CONTRACTION.

A sketch of the computational domain with a visualization of the main boundary conditions especially for air inlets is reported in Fig. 3. Here, the nozzle is partially removed aiming to reduce the overall number of elements and the computational efforts. The air inlets present therefore two different patches, respectively for the outer swirler and the inner one. Also, the position of the flames can be visualized thanks to the isosurfaces of the source term of the progress variable divided over the density (i.e., Production Formation Rate, PFR): it can be observed how the outlet configuration affects the flame shape and the test rig flow-field. Regarding this point, further details will be given in the results section. For the post-processing the *Z-coordinate* indicates the main stream direction while the *X-coordinate* runs through all the burners. For convenience, the origin of the reference frame is set in the top center of the first chamber (upper left in Fig. 3). For all the simulations, as previously mentioned, the experimental rig has been modeled starting from 2 mm upstream of the prefilmer lip up to the burner outlet. A fully unstructured mesh has been generated with polyhedral elements and comprehensive local refinements in the nozzle region and the main reaction zone: an equivalent sizing respectively of 0.3 mm and 0.7 mm has been imposed. Moreover, a buffer zone has been simulated after the outlet section to reproduce the external ambient surrounding and the possible recirculation. Finally, 5 prismatic elements have been used near the walls to obtain an overall number of elements of 18 million. A sketch of the polyhedral mesh for the Inline case is shown in Fig.4. Regarding the two air patches highlighted in Fig. 3 (inner and outlet inlets), a target mass flow rate corresponding to the conditions of Tab.1 has been imposed. This boundary condition consists of an adapted radial profile derived from previously Large Eddy Simulations (LES) carried out on the same nozzle with a smaller effective area [28]. Here, it is assumed that the trend in the radial direction concerning mass flow distribution and turbulent quantities are the same for the two nozzles. Instead, the absolute value of the delivered airflow will be higher for the actual nozzle due to the larger effective area, for the same operating conditions. Therefore, the final profile is up-scaled with to respect the prescribed overall value of air mass flow. These assumptions will be verified and improved once PIV measurements of the injector's flow-field will be available. Moreover, considering the previous studies performed on the single sector configuration by Kasabov [16] for nozzles with different effective areas, only minor discrepancies with the real physics of the problem are expected by following this approach. For the outlet patch, the atmospheric pressure is imposed while all the walls are treated by imposing the no-slip condition for the momentum. For the thermal boundary conditions, due to the influence on the flame, the wall temperature of such walls is set to 1000 K.On the other hand, for the walls in the nozzle region, an adiabatic condition is imposed due to the minor influence on the flame.

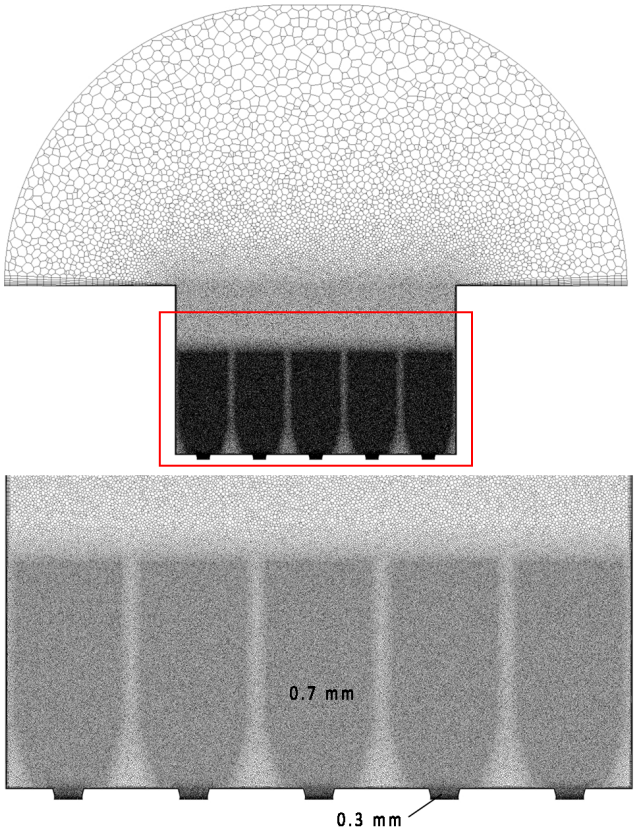

FIGURE 4: MESH GRID FOR THE INLINE CASE.

RESULTS AND DISCUSSIONS

Temperature field

The temperature field is strongly related to the outlet section configuration, especially when the tilt angle is increased. For this reason, the 45° tilt angle has been simulated for both the open and the contraction cases on the outlet plane. In this framework, the presence of an adequate buffer zone beyond the multi-burner casing itself is mandatory, since it allows the reproduction of the recirculation zones observed in the experimental campaign. In Fig 5 the axial velocity is shown for the CFD simulations on the midplane, for both the open case and the one with the contraction and with zero axial velocity isoline superimposed. From this, it can be observed how the presence of the contraction at the outlet is affecting the flow field in the entire burner. Both the configurations reproduce the high-velocity swirling jet issuing from each nozzle. The tilted configuration promotes a cross-flow from the lowest burner to the highest: it can be observed that a non-axisymmetric flow-field is present with respect to each burner axis. This fact can be seen looking to the tip of the swirling jet, now deflected towards the side wall direction, as concluded also

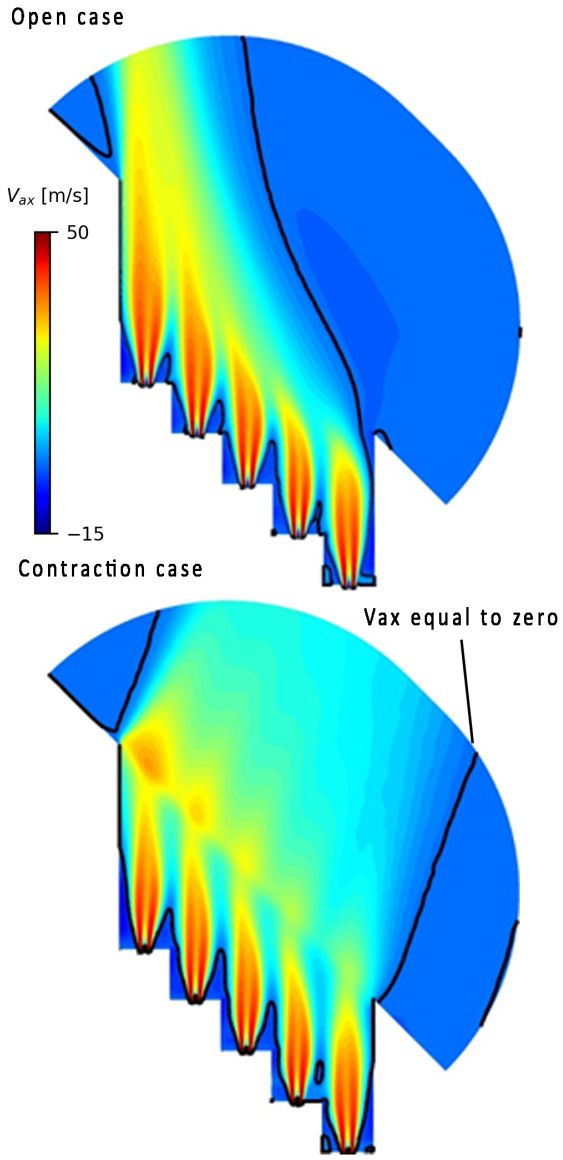

FIGURE 5: AXIAL VELOCITY MAPS FOR THE 45DEG CONFIGURATION. BOTTOM: CONTRACTION CASE. TOP: OPEN CASE. ZERO AXIAL VELOCITY ISOLINES ARE SUPERIMPOSED.

in [24]. Such effect is desired since promotes the hot exhaust gas recirculation, hence the flame stability. On the other hand, a strong three-dimensionality of the flow-field is present, and thus the complexity of the object of study. This fact also highlights that the finite configuration of the test rig has a relevant impact on the final flow field. Concerning this point, by looking at the axial velocity maps for the open case configuration (top contour in Fig 5) the lowest burner is not supplied with a cross-flow by an eventual adjacent burner, so flow separation occurs on the lateral walls. This fact imposes a large recirculation zone that draws air from the outlet section. Again in this picture, considering the case with contraction (bottom contour in Fig 5), it can be seen that the presence of this component influences the flow-field by avoiding the mentioned separation in the final part of the multi-burner. The exhausts are accelerated in the direction normal to the contracted section, hence the ambient air ingestion is avoided [23]. Keeping in mind this, in Fig 6 a comparison between numerical and experimental data in terms of temperature fields at the outlet section and on the diagonal of the 3rd burner is shown respectively for both Inline and 45DEG configurations. Concerning the diagonal plane, experimental measurements have been taken with thermocouples along this direction, between 50 and 250 mm in the axial direction as depicted in the sketch. It can be observed that the low-swirl lifted flame under these operating conditions (i.e., with no preheating) presents a compact inner cold region of the swirling jet, which mixes with the surrounding hot gas downstream, thus reaching higher temperatures. The reaction zones are placed side of the jet in correspondence of the higher temperature regions, as it will be shown in the next paragraph.

The considerations about flow recirculation at the outlet section are confirmed in Fig 6, where the experimental maps of the temperature field on this plane are compared with the numerical results, again for both configurations analyzed for the 45DEG. The open case shows a cold zone in correspondence of the lowest burner, which could not be related to the exhaust gas temperature, but clearly is due to cold ambient air ingestion. Moving to the next burners, the temperature increases, since the effect of the recirculation is less and less visible. This behavior is completely recovered by the CFD simulation, pointing out the capability of the numerical in the reproduction of the main flow-field features occurring here. Similarly, it can be seen how the presence of the contraction leads to a more uniform temperature field, where only minor ingestion of air is present in the proximity of the lowest burner, as highlighted by the lower temperature for the highest part of the outlet. Again, the numerical model is in fair agreement with the experimental measurements, where also here the trend of the temperature is well reproduced moving from the lowest burner to the highest. Some differences between the numerical results and the experimental ones can be observed since a lower temperature is present in the experimental maps near the lowest burner, as well as the peak temperature is higher in this case between the 4th and the 5th burner. Instead, the CFD results are more uniform on all the outlet sections, where peaks of temperature are not reproduced: this behavior could be explained considering the RANS description of the turbulent field, where the effects due to large-scale mixing are underpredicted. The comparison in terms of temperature field on the diagonal plane of the 4th burner for the 45DEG configuration again reproduces

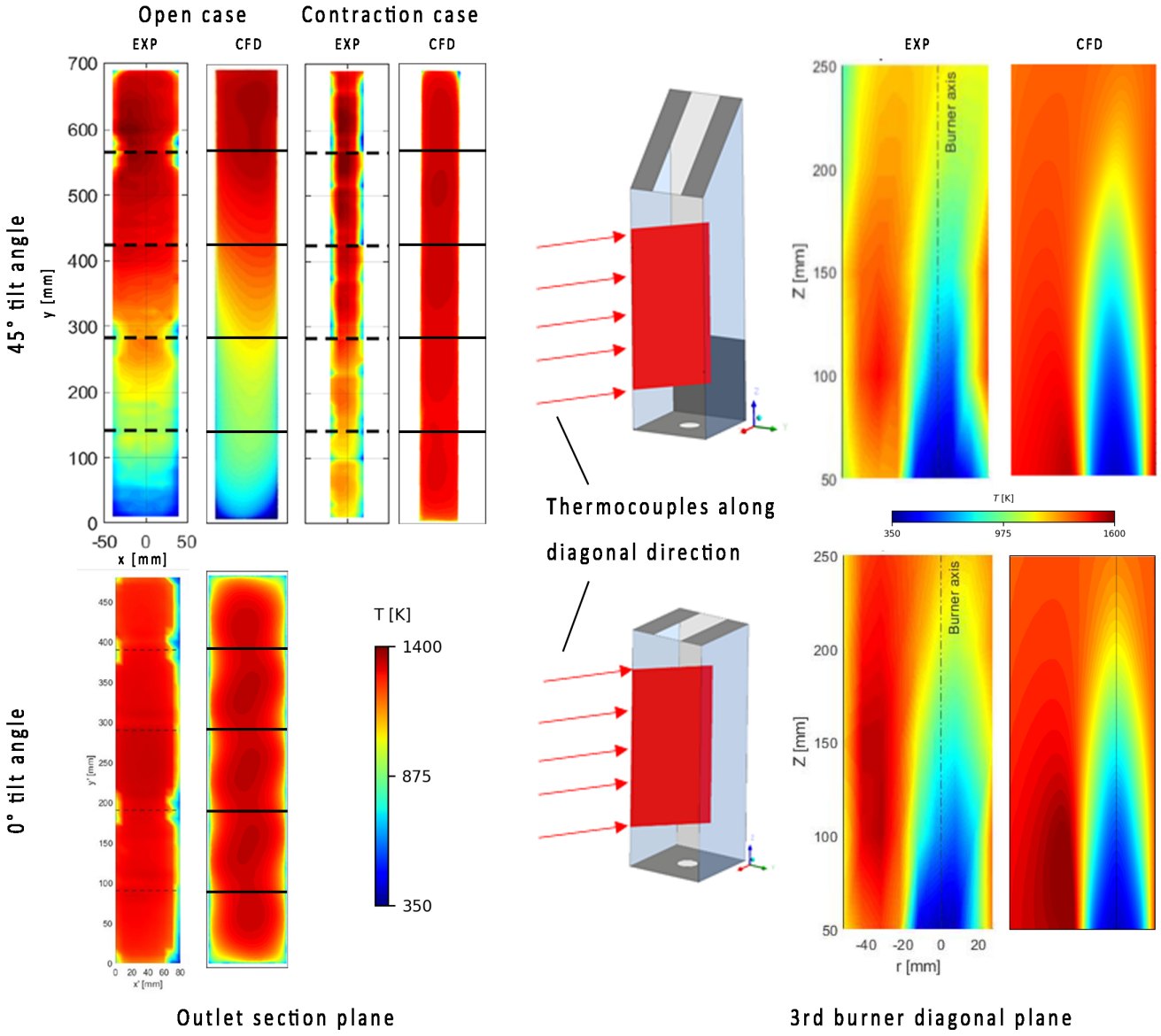

FIGURE 6: COMPARISON BETWEEN CFD AND EXP DATA FOR THE TEMPERATURE FIELD AT THE OUTLET SECTION PLANE AND THE DIAGONAL PLANE FOR BOTH INLINE AND 45DEG CASES.

the cold jet from the nozzle in the proximity of the burner axis: this is affected by the flow deflection previously mentioned, as visible in the EXP map. The CFD simulation is also showing the cold jet structure near the burner axis, but the mixing with the hot exhaust occurs much earlier, and a uniform temperature field can be seen around 250 mm. Also, the jet appears less deflected concerning the experimental results, again due to the limits of the RANS approach in the representation of a swirl-dominated flow. Nevertheless, the main features of the temperature field are reproduced, such as the high-temperature region's side of the cold jet and the cold zone ending at around 140 mm. If the Inline case is considered, for both these planes, the agreement between CFD and experiments is improved with respect of the 45DEG: especially in the diagonal plane, approximately the same length of the coldest zone can be observed, as well as the mixing between cold jet and hot exhaust occurs in the same way around 250 mm. CFD still is missing minor aspects, such as the slight offset of the main jet concerning the burner axis and the lower temper-

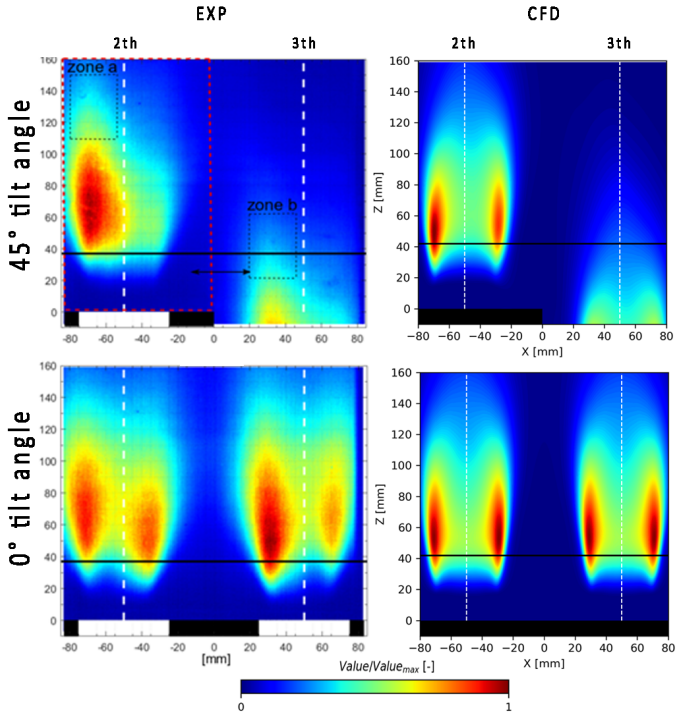

FIGURE 7: COMPARISON (LINE OF SIGHT INTEGRAL) BETWEEN EXPERIMENTAL OH* EMISSION INTENSITY MAP ADAPTED FROM [23] AND PFR MAPS FROM CFD FOR THE 2RD AND 3TH BURNER. TOP: 45DEG. BOTTOM: INLINE.

ature present on the right-side region of the map. These facts could be related again to the RANS description of the flow-field, which mispredicts the swirling flow in the combustion chamber, other than a not optimal description of the thermal wall boundary conditions, affecting the temperature in the side region. Also, It should be noticed that only the open case is present since this layout of the burner does not promote any cross-flow, thus the related recirculation.

OH* chemiluminescence maps

The OH* chemiluminescence maps from the experimental campaign allow to visualize the ongoing reaction occurring in the burner. Since the OH* radical is not present in the employed chemical mechanism, a qualitative comparison is carried out considering the product formation rate previously introduced. Such comparison is often present in the literature since both can be considered indicators of the ongoing reaction. Also, the contours are line-of-sight integrated and the LOH is evaluated as the axial position where the 10% of the global light emission is reached, according to [15, 23]. The comparison between CFD and EXP data is reported in Fig 7: here it is visible the lift-off region devoid of reaction between the flame base and the nozzle exit. The numerical simulations successfully predict the stabilization position of the flames for both configurations, as shown from the LOH around 40 mm. Also, the CFD maps present a misprediction of the spread of the reaction zones due to the RANS approach here employed, which is not correctly reproducing the large-scale mixing and the entrainment of hot combustion products. Nevertheless, considering the Inline rig, the flame shape is fairly well reproduced. An approximately axisymmetric shape can be observed from both numerical and experimental contours, where the main reaction zones are symmetric with respect to the burner's axis, and appears as two different branches occurring on the swirling jet outer shear layer. Instead, the 45DEG case exhibits a strong asymmetry of the main reaction zones with respect to the burner axis. A peak of reaction is present close to the sidewall region, while on the open side it is relatively weak. The simulation seems able to reproduce a reaction peak on the left side of the burner, in agreement with the EXP measurements. However, a non-negligible peak of the reaction is present also in the open side, unlike the experimental measurements. This fact could again be due to the misprediction related to the RANS approach, which is not correctly reproducing the flow field in this region, and thus the effects of the potential wake related to the adjacent sidewall edge. Although this fact, it can be concluded that the numerical model can reproduce some relevant features of the studied flames (e.g., LOH) occurring in the multi-burner configuration, even if some limitations are present due to the modeling strategy applied to the turbulence and the combustion process. As a concluding remark, this numerical setup can be employed effectively to understand the macro effects on the flame interaction due to different tilt angles, while a detailed investigation of the ongoing reactive process will require more complex models and a more detailed description of the boundary conditions.

Tilt angle effects

The numerical models introduced in the previous paragraphs have shown a good agreement with the experimental data, thus justifying the use of the same settings for the investigation of further tilt angles. Since measurements are not available, the idea here is to provide an estimation of the tilt angle impact on the hot gas recirculation through numerical simulations. Considering this, the investigated tilt angles have been the 20° and 30° for the contraction case. In Fig 8, the contour maps corresponding to the 2nd and the 3rd burners are reported in terms of axial velocity and equivalence ratio. Also, the line-of-sight integrated maps of product formation rate normalized over the maximum are shown for the visualization of the reaction zones. Firstly, all the configuration reports the same stabilization position, where the LOH assumes values between 40 and 43 mm. Still considering the previous analysis, the main reaction zones again appear at the side of the swirling jet, but a not trivial behaviour is present con-

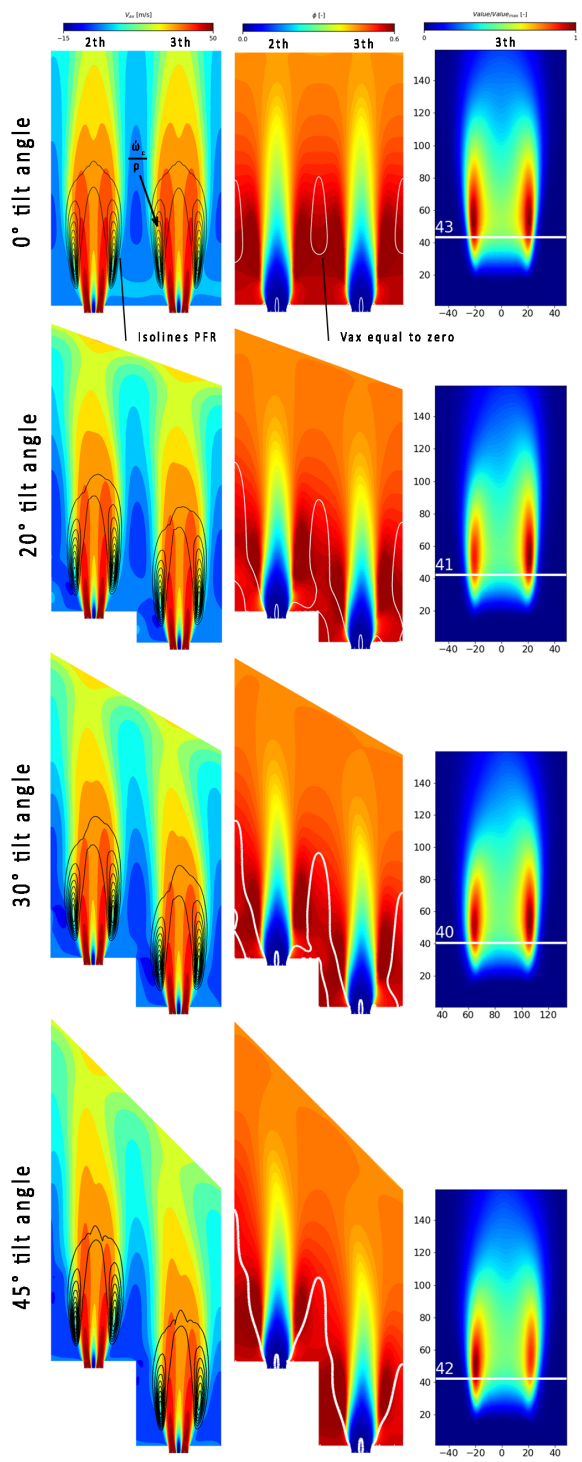

FIGURE 8: CONTOUR MAPS OF AXIAL VELOCITY, EQUIVALENCE RATIO (2RD AND 3RD BURNERS) AND LINE OF SIGHT INTEGRATED MAPS OF PFR (3RD BURNER) FOR THE INVESTIGATED TILT ANGLES. THE NUMBER IN THE FIGURES STANDS FOR THE LOH VALUE IN MM.

cerning the most reactive side. Although the limits pointed out in the previous paragraph concerning the position of these zones, it could be concluded that these regions are related to the outer shear layer between swirling jet and ORZ, as already pointed out in the previous studies for this type of flame on the single sector both experimentally [15] and numerically [28]. This fact could be observed from the axial velocity maps, where the black isolines identify the production formation rate. Accordingly to the line-of-sight-maps, a higher concentration of PFR isolines is present on the outer shear layer, where a high gradient of axial velocity is present. This is true for all the configurations, where the main difference concern only the shape and extension of the recirculation zones, as depicted from the zero axial velocity isolines superimposed on the equivalence ratio maps. An interesting finding is that the ORZ is not only present in correspondence of the sidewall, but also on the open side, and seems to interact with the lower burner with a backward transport of combustion products. This very particular situation is present for each tilt angle and could be related to the strong three-dimensionality of the flow field for this test rig. Eventually, also the Inline case, which should not present any ORZ occurrence due to the absence of walls for this view is showing some recirculation zones. Again this fact could be explained considering the presence of complex recirculation zones due to the optical windows. Another very important point is the fact that the 45DEG configuration, which was described in the previous work on the SHC concept [21] as the most promising in terms of flame stability, with this kind of nozzle and at least the present operating conditions is exhibiting an overall lower value of equivalence ratio, thus vitiated products transport. This fact seems related to a specific operational mode, where the flame actually is less interacting with the next burner and the sidewall operates as a barrier among burners, similarly to what has been observed in [22] for high-swirl injectors.

This point could be observed also in Fig 9, where the equivalence ratio, the temperature, and the x velocity components are reported for the planes of the interface between the 2nd and 3rd burners. It should be noticed that according to the reference system reported in the test case section, a negative value of the x velocity is associated with the mass flow from the lower burner to the higher one. Also, for each map, the dashed line represents the position of the sidewall edge. It can be observed that the Inline case has a strong presence of hot vitiated products on these interfaces, at an axial position approximately in correspondence of the flame position. The absence of the sidewall helps in this sense, but at the same time a very little transverse transport is present, as can be seen from the x velocity map, where low values are assumed on this plane. Nevertheless, it is interesting to see that is anyway present a transport of recirculating products entering the plane between 0 a 50 mm, and vice versa on the other side, due to the swirled flow field of each burner.
The situation is reverted if the 45DEG configuration is considered. A strong transverse transport is present, promoting a mass

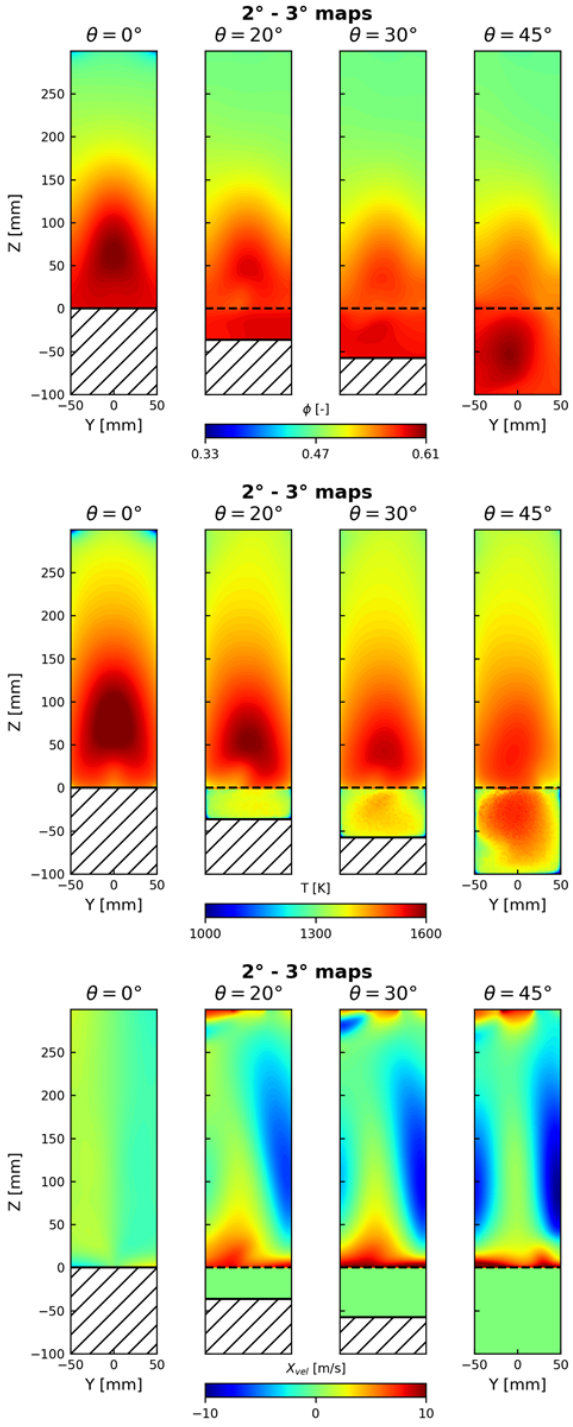

FIGURE 9: CONTOUR MAPS OF EQUIVALENCE RATIO, TEMPERATURE AND X-VELOCITY ON THE INTERFACE PLANES BETWEEN 2ND AND 3RD BURNERS, FOR THE INVESTIGATED TILT ANGLES. THE DASHED HORIZONTAL LINE IS THE SIDE WALL HEIGHT.

flow from the lower burner to the higher one in the proximity of the optical windows. As already pointed out in Fig 8, a backward component of velocity is present near the sidewall edge, moving combustion products back to the lower burner. However, this configuration for the present operating conditions seems less functional, since the hot combustion products remain confined below the sidewall edge, hence limiting the interaction among adjacent burners. Finally, the 20DEG and the 30DEG are a sort of trade-off between the previously described configuration. An appreciable cross-flow is present according to the velocity maps. Also, the velocity is assuming a higher value between 0 and 50 mm, where the tangential flow of two consecutive burners is coherent, while it is weakened between -50mm and 0 mm, where these two fields are interacting one against the other. Also, the higher values of equivalence ratios, therefore of the vitiated products are above the sidewall edge and similarly the temperature field. This points out that these lower values of the tilt angle could be more suitable for the application of the CHAiRLIFT concept.

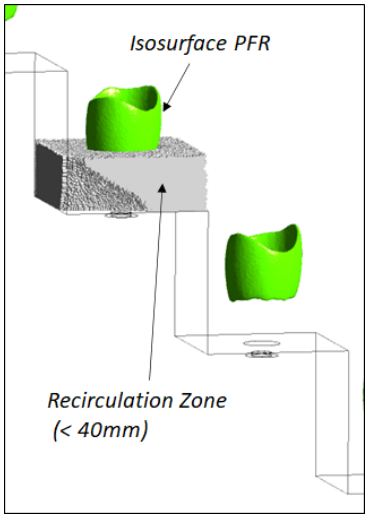

FIGURE 10: RECIRCULATION ZONES SKETCH WITH ISOSURFACES OF PRODUCTION FORMATION RATE (45DEG CASE).

Finally, some consideration can be drawn considering a series of parameters for evaluating the performance of the configuration numerically investigated so far. In this fashion, the extension of the recirculation zones as well as the volume averaged temperature in these regions is evaluated for the tested tilt angles: these data are reported . Also, only such regions included within 40mm from the burner dome are considered, therefore in the lift-off region, as depicted in Fig 10. It is expected that these zones act as a reservoir of hot vitiated products and participate in

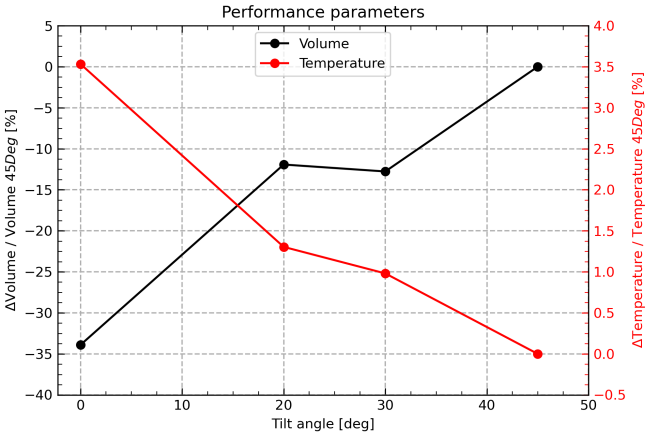

V

FIGURE 11: RECIRCULATION ZONES EXTENSION AND RELATED VOLUME AVERAGED TEMPERATURE FOR THE INVESTIGATED TILT ANGLES (VARIATION WITH RESPECT TO 45° TILT ANGLE).

flame stabilization. Moreover, only the mid burner is considered, assuming it could be considered as the one less influenced by the lateral confinement.

The results are reported Fig 11 as variation from the 45DEG value, and adimensionalized over the same value. These results confirm the previous observation since the Inline case has the smallest extension of the recirculation regions but also the highest temperature with respect to the 45DEG configuration. The 20DEG and 30DEG cases are instead comparable and present a good extension of the recirculation zones, especially with respect to the Inline case. Meanwhile, also the average temperature is better than the 45DEG configuration, even if not so far from this value.

CONCLUSIONS

In the present work the CHAiRLIFT test rig in multi-burner configuration is numerically investigated for different values of the tilt angle. The whole rig has been modeled in order to understand the mutual interaction of adjacent flames when low-swirl lean lifted spray flames are arranged with a tilted layout of the burners. Two configurations, Inline and 45DEG case, have been validated against the available experimental data in terms of OH* chemiluminescence maps and temperature fields. Also, further tilting angles between these two reference values have been investigated from the numerical point of view. These studies have shown that the numerical modeling strategy, allows reaching a good agreement with the experimental data when the full rig configuration is considered. The numerical simulations point out that tilting angles between 20° and 30° could lead to a stronger recirculation and in general better flame stability. Also, a further improvement will be represented by the review of the employed boundary conditions once PIV measurement of the flowfield will be available from the ongoing experimental activity.

ACKNOWLEDGMENT

This project has received funding from the Clean Sky 2 Joint Undertaking (JU) under grant agreement N. 831881 (CHAiRLIFT). The JU receives support from the European Union's Horizon 2020 research and innovation program and the Clean Sky 2 JU members other than the Union.

The authors acknowledge the CINECA award under the ISCRA initiative, for the availability of high-performance computing resources. Dr. S. Harth and M. Shamma are gratefully acknowledged for the availability of the test rig measurements.

REFERENCES

[1] Grewe, V., Rao, A. G., Grönstedt, T., Xisto, C., Linke, F., Melkert, J., Middel, J., Ohlenforst, B., Blakey, S., Christie, S., et al., 2021. "Evaluating the climate impact of aviation emission scenarios towards the paris agreement including covid-19 effects". *Nature Communications,* ***12***(1), pp. 1–10.

[2] Darecki, M., Edelstenne, C., Enders, T., Fernandez, E., Hartman, P., Herteman, J., Kerkloh, M., King, I., Ky, P., Mathieu, M., et al., 2011. "Flightpath 2050: Europe's vision for aviation: Report of the high level group". *Publications Office of the European Union: Luxembourg*.

[3] Nojoumi, H., Dincer, I., and Naterer, G., 2009. "Greenhouse gas emissions assessment of hydrogen and kerosene-fueled aircraft propulsion". *International journal of hydrogen energy,* ***34***(3), pp. 1363–1369.

[4] Yılmaz, İ., İlbaş, M., Taştan, M., and Tarhan, C., 2012. "Investigation of hydrogen usage in aviation industry". *Energy conversion and management,* ***63***, pp. 63–69.

[5] Yilmaz, N., and Atmanli, A., 2017. "Sustainable alternative fuels in aviation". *Energy,* ***140***, pp. 1378–1386.

[6] Amerini, A., Langone, L., Vadi, R., and Andreini, A., 2021. "Assessment of a hybrid propulsion system for short-mid range application with a low-order code". In E3S Web of Conferences, Vol. 312, EDP Sciences, p. 11005.

[7] Lefebvre, A. H., and Ballal, D. R., 2010. *Gas turbine combustion: alternative fuels and emissions*. CRC press.

[8] Liu, Y., Sun, X., Sethi, V., Nalianda, D., Li, Y.-G., and Wang, L., 2017. "Review of modern low emissions combustion technologies for aero gas turbine engines". *Progress in Aerospace Sciences,* ***94***, pp. 12–45.

[9] Ranasinghe, K., Guan, K., Gardi, A., and Sabatini, R., 2019. "Review of advanced low-emission technologies for sustainable aviation". *Energy,* ***188***, p. 115945.

[10] `https://cordis.europa.eu/project/id/831881/en`.

[11] Lawn, C., 2009. "Lifted flames on fuel jets in co-flowing air". *Progress in Energy and Combustion Science,* ***35***(1), pp. 1–30.

[12] Lyons, K. M., 2007. "Toward an understanding of the stabilization mechanisms of lifted turbulent jet flames: experiments". *Progress in Energy and Combustion Science,* ***33***(2), pp. 211–231.

[13] Day, M., Tachibana, S., Bell, J., Lijewski, M., Beckner, V., and Cheng, R. K., 2012. "A combined computational and experimental characterization of lean premixed turbulent low swirl laboratory flames: I. methane flames". *Combustion and Flame,* ***159***(1), pp. 275–290.

[14] Shahsavari, M., Farshchi, M., and Arabnejad, M. H., 2017. "Large eddy simulations of unconfined non-reacting and reacting turbulent low swirl jets". *Flow, Turbulence and Combustion,* ***98***(3), pp. 817–840.

[15] Kasabov, P., Zarzalis, N., and Habisreuther, P., 2013. "Experimental study on lifted flames operated with liquid kerosene at elevated pressure and stabilized by outer recirculation". *Flow, turbulence and combustion,* ***90***(3), pp. 605–619.

[16] Kasabov, P., 2014. "Experimentelle untersuchungen an abgehobenen flammen unter druck". PhD thesis.

[17] Lefebvre, A. H., and McDonell, V. G., 2017. *Atomization and sprays*. CRC press.

[18] Fokaides, P., and Zarzalis, N., 2007. "Lean blowout dynamics of a lifted stabilized, non-premixed swirl flame". In Proceedings of European Combustion Meeting, Vol. 7, p. 2.

[19] Fokaides, P. A., Kasabov, P., and Zarzalis, N., 2008. "Experimental investigation of the stability mechanism and emissions of a lifted swirl nonpremixed flame". *Journal of engineering for gas turbines and power,* ***130***(1).

[20] Sedlmaier, J., Habisreuther, P., Zarzalis, N., and Jansohn, P., 2014. "Influence of liquid and gaseous fuel on lifted flames at elevated pressure stabilized by outer recirculation". In Turbo Expo: Power for Land, Sea, and Air, Vol. 45684, American Society of Mechanical Engineers, p. V04AT04A054.

[21] Ariatabar, B., Koch, R., Bauer, H.-J., and Negulescu, D.-A., 2016. "Short helical combustor: Concept study of an innovative gas turbine combustor with angular air supply". *Journal of Engineering for Gas Turbines and Power,* ***138***(3).

[22] Hu, B., Zhang, J., Deng, A., Zhao, W., and Zhao, Q., 2018. "Numerical investigation on single-restricted swirling flows in an innovative combustor". In Turbo Expo: Power for Land, Sea, and Air, Vol. 51067, American Society of Mechanical Engineers, p. V04BT04A002.

[23] Shamma, M., Hoffmann, S., Harth, S. R., Zarzalis, N., Trimis, D., Koch, R., Bauer, H.-J., Langone, L., Galeotti, S., and Andreini, A., 2021. "Investigation of adjacent lifted flames interaction in an inline and inclined multi-burner arrangement". In Turbo Expo: Power for Land, Sea, and Air, Vol. 84959, American Society of Mechanical Engineers, p. V03BT04A020.

[24] Hoffmann, S., Koch, R., and Bauer, H.-J., 2021. "Numerical investigation of the low-swirl flow in an aeronautical combustor with angular air supply". In Turbo Expo: Power for Land, Sea, and Air, Vol. 84928, American Society of Mechanical Engineers, p. V02CT34A019.

[25] ANSYS, 2019. *Fluent 19.3 Theory Guide*.

[26] Luche, J., Reuillon, M., Boettner, J.-C., and Cathonnet, M., 2004. "Reduction of large detailed kinetic mechanisms: application to kerosene/air combustion". *Combustion science and technology,* ***176***(11), pp. 1935–1963.

[27] Gepperth, S., Koch, R., and Bauer, H.-J., 2013. "Analysis and comparison of primary droplet characteristics in the near field of a prefilming airblast atomizer". In Turbo Expo: Power for Land, Sea, and Air, Vol. 55102, American Society of Mechanical Engineers, p. V01AT04A002.

[28] Langone, L., Sedlmaier, J., Nassini, P. C., Mazzei, L., Harth, S., and Andreini, A., 2020. "Numerical modeling of gaseous partially premixed low-swirl lifted flame at elevated pressure". In Turbo Expo: Power for Land, Sea, and Air, Vol. 84133, American Society of Mechanical Engineers, p. V04BT04A068.